RESEARCH ARTICLE

A Case Study on Statistical Analysis of Geomagnetic Storm 3-5 August 2010

Z. Can[1*], and H. Ş. Erdağ[2]

[1]Yıldız Technical University, Faculty of Art and Sciences, Department of Physics, Davutpaşa, 34220, İstanbul, Türkiye
[2]Gebze Technical University, Faculty of Science, Department of Physics, 41400, Gebze, Kocaeli, Türkiye

ABSTRACT

The solar flare that occurred on August 1, 2010, was a powerful event that led to the interaction of two coronal mass ejections (CMEs), resulting in a significant CME-CME eruption. This eruption struck Earth on August 3, causing a major geomagnetic storm that had widespread impacts on Earth's magnetic environment. Detecting geomagnetic storms is essential for safeguarding space missions, satellite operations, and communications systems. Failure to accurately predict these storms can disrupt critical infrastructure. The CME-CME interaction in August 2010 differs from ordinary CMEs in terms of particle velocity and density, which were observed to reach unprecedented levels during this event. In this study, a statistical model using the multiple linear regression method was developed to examine the effects of CME-CME interaction on Earth's magnetic field by utilizing characteristics such as particle velocity (v) and density (Np). The study evaluated the effects of solar parameters during G3 and G2-level geomagnetic storms. It was found that particle density significantly increases the intensity and duration of geomagnetic storms, whereas particle velocity notably reduces these effects, exhibiting an opposing influence.

Keywords: Geomagnetic storm; coronal mass ejection; CME-CME interaction; regression; statistical analysis; space weather.

1. INTRODUCTION

Space weather has gained traction as an important area of study in recent years, continuing a long tradition of scientific research to understand processes occurring in the Earth's near-space environment. Space weather refers to the collective results and effects of a series of physical phenomena originating from the Sun and propagating through the interplanetary environment. Magnetic field disruptions on the Sun give rise to sunspots - dark regions on the Sun's surface (photosphere) that are cooler than their surroundings. These spots are caused by twisted magnetic fields. They create active regions that can produce solar flares. Active regions can also eject magnetized plasma at high speeds. This plasma can travels through interplanetary space. This plasma ejection into the interplanetary region is called a Coronal Mass Ejection (CME). If CMEs are released consecutively and the trailing CME catches up with the preceding one, the event is referred to as a CME-CME interaction or cannibalistic CME (Chattopadhyay & Khondekar 2023). The merging of these large-scale magnetic structures, carrying ionized plasma, leads to a buildup at the front of the CME. The interaction between the two magnetized plasma systems further complicates the structure (Gopalswamy 2001). Moreover, energy stored in twisted magnetic fields above sunspots can be abruptly released, causing solar flares-phenomena that often occur alongside various solar events (gsfc.nasa.gov).

On August 1, 2010, sunspot 1092 produced a C3-class solar flare, accompanied by the eruption of a massive magnetic filament across the Sun's northern hemisphere. These events, likely connected by long-range magnetic fields, merged to form a CME-CME interaction, recorded by NASA's Solar Dynamics Observatory. Figure 1 is a visual representation of the Sun during this event, highlighting sunspot 1092 and resulting flare. This event struck Earth in the evening hours of August 3 and caused a significant disturbance in Earth's magnetic field (magnetosphere), resulting in a geomagnetic storm. The detection and understanding of geomagnetic storms are crucial due to their impact on modern processes such as space missions, satellite safety, atmospheric processes, and communication. If a second CME, ejected from a region near the first, moves faster than the initial CME, it will overtake and engulf it. Thus, this formation, which is formed by the interaction of two CMEs and is called a cannibal CME, has a more complex structure than typical CMEs. Since these cannibal CMEs are the combination of two different coronal mass ejections, they are larger and more complex than typical CMEs in terms of speed and intensity. The August 2010 storm exemplifies a cannibalistic CME, exhibiting the distinctive characteristics. Parameters such as the velocity, pressure, and density of particles from the Sun, as well as the direction of the interplanetary magnetic field, play a significant role in the formation of geomagnetic storms. In this
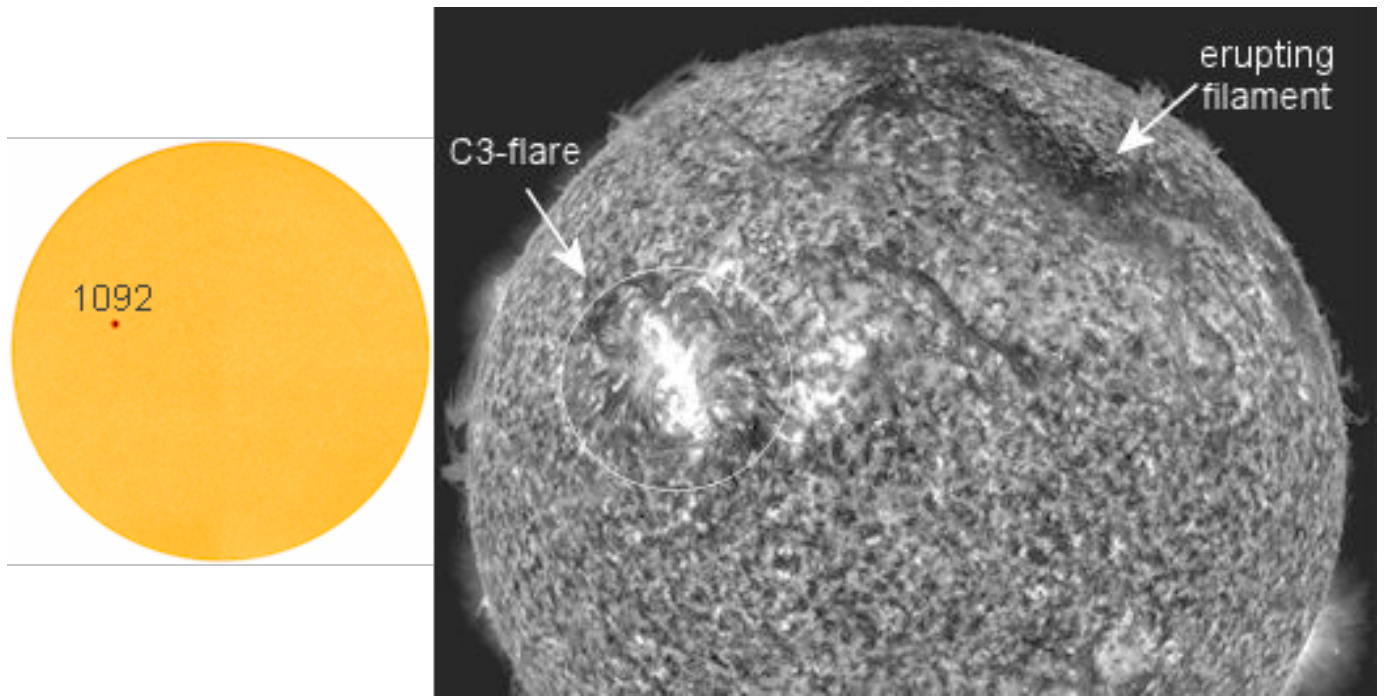
Figure 1. *S*unspot number 1092 and the resulting flare (Space Weather 2024).

study, we utilized particle velocity (v) and density (Np)—the two distinguishing features of the cannibalistic CME compared to other ejections and solar winds. To reveal the effects of solar parameters on Earth's magnetic field during the consecutive G3 (strong geomagnetic storms with a Kp index between 7 and 8 and a Dst index between -100 nT and -250 nT) and G2 (moderate geomagnetic storms with a Kp index between 6 and 7 and a Dst index between -50 nT and -100 nT) level geomagnetic storms, we developed a statistical model.

Table 1. G, Kp, and Dst index ranges corresponding to various storm levels.

Geomagnetic Storm	G Index	Kp Range	Dst Range
Quite Day	G0	Kp< 5	$-30 <$ Dst
Weak	G1	$5 \le$Kp< 6	$-50 <$ Dst ≤ -30
Moderate	G2	$6 \le$Kp< 7	$-100 <$ Dst ≤ -50
Strong	G3	$7 \le$Kp< 8	$-250 <$ Dst ≤ -100
Severe	G4	$8 \le$Kp< 9	$-500 <$ Dst ≤ -250
Extreme	G5	Kp$\ge$ 9	Dst $\le$-500

2. DATA

The Dst index is the most widely used measure for classifying geomagnetic storms. If the Dst peak value is between -30 and -50 nT, the storm is classified as weak; if the Dst peak value is between -50 and -100 nT, it is considered a moderate storm; and if the Dst peak value falls below -100 nT, it is categorised as an intense storm (Prestes et al. 2017; Gonzalez et al. 1994). Geomagnetic storms are also classified based on the planetary K index (Kp), which defines the intensity of the disturbance. The Kp index ranges from 0 (very quiet) to 9 (very disturbed) and is related to 28 different values: 0, 0+, 1-, 1, 1+, ..., 9-, 9 (Bartels 1949). When the Kp value is five or higher, it is represented by the geomagnetic storm index G. The classification of geomagnetic activity according to G, Kp, and Dst ranges, as defined by the National Oceanic and Atmospheric Administration (NOAA) Space Weather Prediction Center (SWPC), is shown in Table 1 (Chakraborty & Morley 2020).

Particle velocity data from the Sun were obtained using the *WIND* satellite. Velocity and density data were collected hourly

during the three-day storm. The independent variables represent the magnitude of particle velocity (v) and the proton density of the ejection (Np). In this way, matching hourly datasets for both v and Np were created. The Dst index was selected as the dependent variable to observe the variability in Earth's magnetic field. The primary reason for choosing the Dst index is its availability as hourly data, which aligns with the other variables. We obtained the Dst index data from the World Data Center for Geomagnetism, Kyoto (Kyoto University 2024). This database provides hourly Dst index values derived from geomagnetic observations collected by a global network of observatories. A disturbance in Earth's magnetic field is classified as a geomagnetic storm if the CME value exceeds -30 nT. Once this threshold is crossed, the day is no longer considered quiet but instead marked as the onset of a geomagnetic storm.

We used a multiple linear regression model to analyze the August 2010 ejection that caused the geomagnetic storm. The independent variables in the model were the particle velocity and particle density of the CME-CME interaction, while the dependent variable was the Dst index, which indicates the
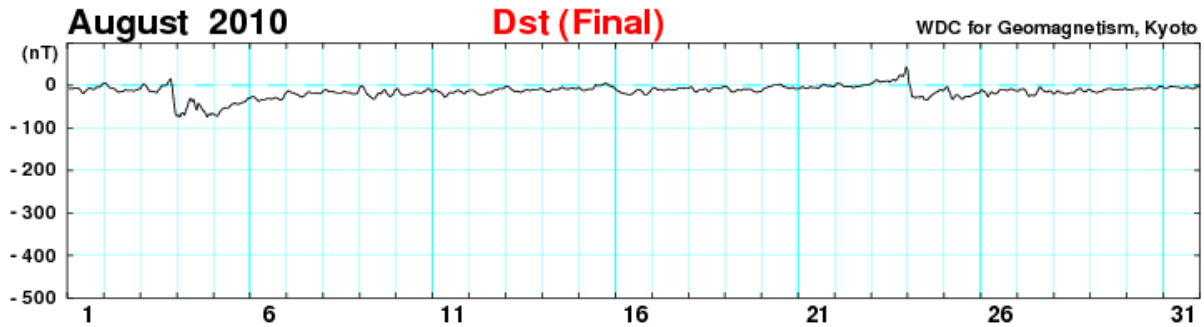
Figure 2. Dst index variation during August 2010.

disturbance in Earth's magnetic field. In the model, the quiet hours of the 3-5 August storm were identified, and a dummy variable was included for the hours when the storm occurred. In this way, the anomalous behavior in the magnetosphere was introduced into the model through the dummy variable.

Linear relationships between Earth's magnetic field and solar parameters were examined. Independent variables with no high correlation between them were selected. Multiple linear regression model tests were applied in the SPSS software for the independent variables (v, Np) and the dependent variable Dst. The significance of the model was evaluated through the model's result tables. The F-test was used to check if at least one variable in the model was significant (Table 2). Subsequently, it was confirmed that the significance values for each statistically significant independent variable fell within the confidence interval. To assess how were the changes in the dependent variable were explained, the R and R^2 values were obtained. The multiple linear regression model, using 70 data points for each variable, was constructed in the following equation form.

$$Y = \beta_0 + \beta_1 X_1 + \beta_2 X_2 + \beta_3 D_1 \tag{1}$$

where Y represents the dependent variable, Dst, while X values represent v and Np, respectively, and D represents the dummy variable. Here, the β values are the constant coefficients that will be obtained from the model for each variable.

3. RESULTS

Several (five) coronal mass ejections (CMEs) occurred from regions on the Earth-facing surface of the Sun. Two of the CMEs, ejected from the widespread and highly complex sunspot AR1092 on August 1, 2010, interacted and merged with each other, forming a magnetic structure known as a cannibalistic CME (or CME-CME, Temmer et al. 2012; Vrsnak 1992; Vršnak & Gopalswamy 2002). Additionally, a solar flare, a solar tsunami, the ejection of numerous magnetic filaments from the Sun's surface, large-scale oscillations of the solar corona, and radio bursts were detected. Upon ejections from the Sun, the CME interacts with the interplanetary medium, transferring energy and momentum through magnetohydrodynamic (MHD)

waves (Jacques 1977). Figure 2 shows the Dst index variation for the month of August.

The CMEs ejected into interplanetary space by this complex eruption impacted Earth's magnetic field on August 3 and 4, which causing geomagnetic storms. The storm triggered by the CME-CME interaction caused the Dst index to drop to a value of -74 nT. Based on the Kp index calculated from Potsdam (located in Germany and home to the GFZ German Research Centre for Geosciences), we classified the August 3 storm as G3 and the August 4 storm as G2.

Figure 3 shows the variations in solar wind parameters from August 2-6, 2010, covering the period before, during, and after the geomagnetic storm. We used data from the *WIND* satellite, which is designed to provide information on the characteristics of the interplanetary magnetic field. The data obtained from the *WIND* satellite, listed from top to bottom, include the solar wind magnetic field strength (B), the z-component of the magnetic field (Bz), the magnitude of the solar wind speed (v), proton number density (Np), the solar wind ram pressure calculated from field and plasma parameters (Psw), and Akasofu's epsilon parameter (ε; 10^{11} W), which measures the energy transferred to Earth's magnetosphere. The data were obtained from the *WIND* satellite in the Geocentric Solar Magnetospheric (GSM) coordinate system and at high resolution (with 1-minute intervals) for detailed analysis.

As seen in Figure 3, the z-component of the magnetic field exhibited fluctuations within a range of approximately 30 nT. Before the storm, the solar wind speed was around 400 km s^{-1}, but with the onset of the storm, the speed increased by approximately 200 km s^{-1}, reaching 600 km s^{-1}. The particle number density rose to about 25 particles per cubic centimeter. The solar wind pressure also increased, reaching a value of approximately 18 nPa. During the storm, the ε parameter, measuring energy transfer from the solar wind to the environment, reached 20×10^{11} W.

The statistical model developed using the regression method was applied to the geomagnetic storm that occurred on August 3-5, 2010. In the model, where the confidence interval was set at 95%, the F-test resulted in a value less than 0.05 (Table 2). The model's outputs show that the R value, indicating the correlation between the dependent and independent variables, was
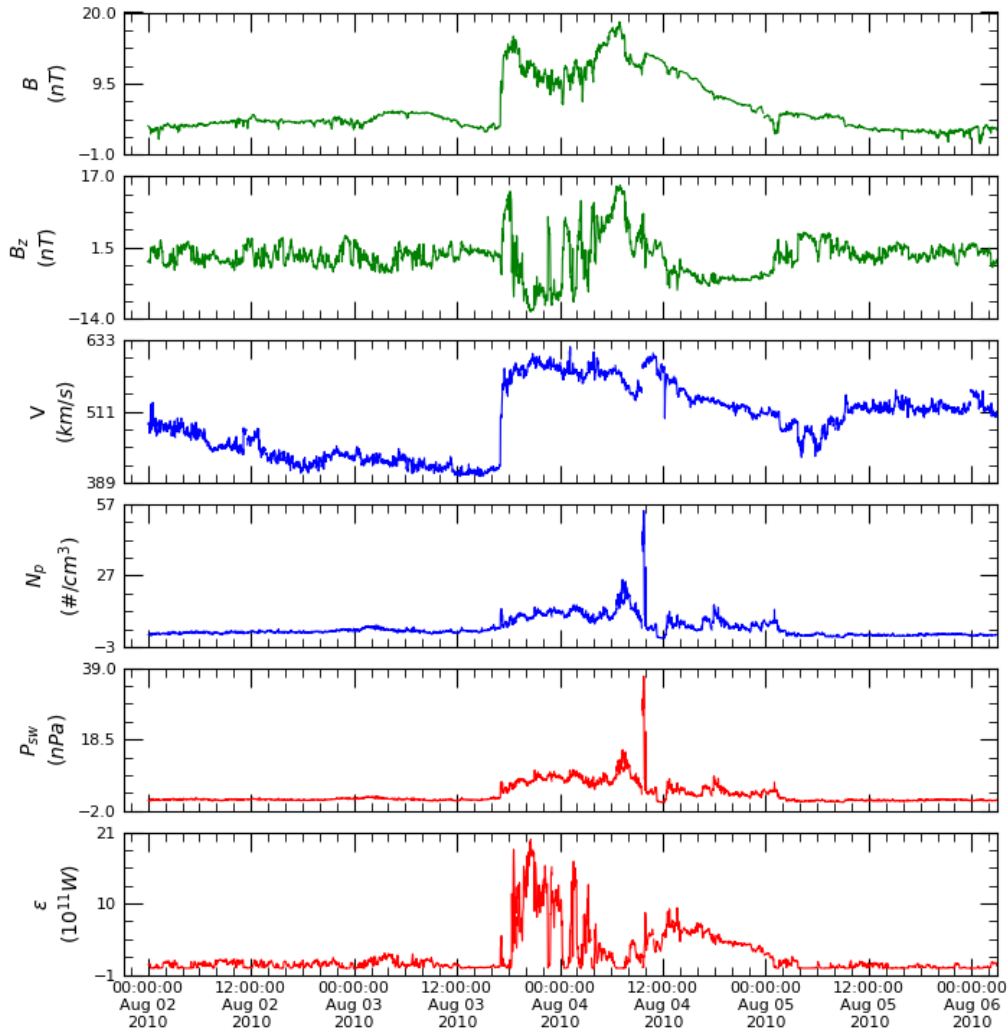
Figure 3. *Variations in solar wind parameters from the WIND satellite between August 2-6, 2010: B (magnetic field), Bz (component), v (magnitude of solar wind speed), Np (particle number density), and ε (Akasofu's epsilon parameter).*

91.5%. Similarly, the R-squared value was found to be 83.7%, which is quite high. This R-squared value demonstrates that 83.7% of the variation in the dependent variable is explained by the independent variables. The coefficients obtained during the storm period indicate the effect of the velocity and density of the cannibalistic CME on the dependent variable, the Dst value. The beta coefficients are 0.156 for the CME-CME ejection velocity and -2.516 for the particle density. The significance values for the independent variables were found to be below 0.05.

4. CONCLUSION AND DISCUSSION

A statistically significant model was obtained for the August 3-5 geomagnetic storm using the developed statistical model.

Table 2. Statistical model results of the regression analysis applied to the geomagnetic storm of August 3-5, 2010.

F Test	R	R^2	β for v	β for Np	Sig. for v	Sig. for Np
<0.001	0.915	0.837	0.156	-2.516	<0.001	<0.001

The F-test of the model resulted in a value well below 0.05, as expected, demonstrating that at least one of the independent variables significantly explains the variation in the dependent variable. However, the key point is to observe the significant effect of both independent variables on the dependent variable. For this, the significance values of each independent variable in the model must be below 0.05. The significance values for each independent variable used in the geomagnetic storm model meet the required condition, allowing for the interpretation of

other model values. The high R value of 91.5% indicates that the selected independent variables are the most ideal for explaining the dependent variable. For the model to be successful, the independent variables must explain the variability in the dependent variable as much as possible. Here, the R-squared value of 83.7% shows that the independent variables in the model successfully explain the variability in the dependent variable. These results highlight the significant role of particle velocity and density among the ejection parameters as the primary sources of the geomagnetic storms and disturbances in Earth's magnetic field.

The statistical model developed in this study underscores that the velocity and density of the CME-CME ejection responsible for the August storm are key factors driving the storm. Based on the beta coefficients in the model, the following can be stated for each parameter: as the density of the CME-CME ejection increases, the Dst values of the resulting geomagnetic storm tend to shift towards more negative values. This plays a crucial role in increasing the strength (class) and duration of the geomagnetic storm, extending both the main phase and the recovery phase of the storm. However, the opposite is observed for particle velocity. As the unit velocity increases during the storm, the Dst value moves toward more positive values. Consequently, the storm's intensity decreases, and the storm duration shortens, allowing a quicker transition to a quiet day. An average unit change in density decreases the Dst value by -2.516 nT, while an average unit change in velocity increases the Dst by 0.156 nT. As seen in Figure 3 (speed and density graph numbers), specifically in the 3rd and 4th graphs from the bottom to the top, the significant variations in speed and density indicate that the coefficients of these variables have a substantial impact on the geomagnetic storm class and, consequently, on Earth's magnetic field.

These magnetic field disturbances in Earth's magnetic field can also affect the Earth's ionosphere, which is known as a natural plasma laboratory. This complex storm has been investigated by Valladares et al. (2017). They observed that during the storm, the Total Electron 157 Content (TEC) significantly increased at mid-latitudes. During the storm, the Kp index was 2 on August 2, 7- on August 3, 6+ on August 4, 4 on August 5, and 2+ on August 6. Accordingly, a G3 (strong) level storm occurred on August 3, and a G2 (moderate) level storm occurred on August 4. By August 5, conditions had returned to a quiet day. During the G3 (strong) level storm, voltage corrections may be required, surface charging of satellite components may occur, drag on low-Earth orbit satellites may increase, and attitude correction may be necessary. Additionally, satellite navigation and low-frequency radio navigation issues may arise.In conclusion, in order to minimize the serious effects of the disturbances in the Earth's magnetic field caused by geomagnetic storms on satellite operations, navigation systems and communication infrastructures, the dynamics of geomagnetic storms should be examined in more detail and comprehensively.

LIST OF AUTHOR ORCIDS

Z. Can   https://orcid.org/0000-0002-3039-7454

H. Ş. Erdağ   https://orcid.org/0000-0003-4584-8497

REFERENCES

Bartels J., 1949, IATME Bulletin, 12b, 97

Chakraborty S., Morley S. K., 2020, Journal of Space Weather and Space Climate, 10, 36

Chattopadhyay A., Khondekar M., 2023, Astronomy and Computing, 43, 100695

Gonzalez W. D., Joselyn J. A., Kamide Y., Kroehl H. W., Rostoker G., Tsurutani B. T., Vasyliunas V. M., 1994, Journal of Geophysical Research: Space Physics, 99, 5771

Gopalswamy 2001, The Astrophysical Journal, 548, l91

Jacques S. A., 1977, The Astrophysical Journal, 215, 942

Kyoto University 2024, World Data Center for Geomagnetism, Kyoto. Kyoto University, https://wdc.kugi.kyoto-u.ac.jp/dstdir/

Prestes A., Klausner V., González A. O., Serra S. L., 2017, Advances in Space Research, 60, 1850

Space Weather 2024, Space Weather: News and Information about the Sun-Earth Environment, https://www.spaceweather.com/

Temmer M., et al., 2012, The Astrophysical Journal, 749, 57

Valladares C. E., Eccles J. V., Basu S., Schunk R. W., Sheehan R., Pradipta R., Ruohoniemi J. M., 2017, Journal of Geophysical Research: Space Physics, 122, 3487

Vrsnak B., 1992, Annales Geophysicae, 10, 344

Vršnak B., Gopalswamy N., 2002, Journal of Geophysical Research: Space Physics, 107, SSH 2